

The mass assembly history of black holes in the Universe

Priyamvada Natarajan

Department of Astronomy, Yale University, 260 Whitney Avenue, New Haven CT 06511

Abstract. We track the growth and evolution of high redshift seed black holes over cosmic time. This population of massive, initial black hole seeds form at these early epochs from the direct collapse of pre-galactic gas discs. Populating dark matter halos with seeds formed in this fashion, we follow their mass assembly history to the present time using a Monte-Carlo merger tree approach. Using this formalism, we predict the black hole mass function at the present time; the integrated mass density of black holes in the Universe; the luminosity function of accreting black holes as a function of redshift and the scatter in observed, local $M_{\text{bh}} - \sigma$ relation. Signatures of these massive seed models appear predominantly at the low mass end of the present day black hole mass function. In fact, our prediction of the shape of the $M_{\text{bh}} - \sigma$ relation at the low mass end and increased scatter has recently been corroborated by observations. These models predict that low surface brightness, bulge-less galaxies with large discs are least likely to be sites for the formation of massive seed black holes at high redshifts. The efficiency of seed formation at high redshifts also has a direct influence on the black hole occupation fraction in galaxies at $z = 0$. This effect is more pronounced for low mass galaxies today as we predict the existence of a population of low mass galaxies that do not host nuclear black holes. This is the key discriminant between the models studied here and the Population-III remnant seed model.

Keywords: Cosmology, Black holes, Quasars, Galactic Nuclei

PACS: 98.62.Js, 98.54.-h, 98.54.Aj

INTRODUCTION

The demography of nearby galaxies suggests that most of them harbor a quiescent super-massive black hole (SMBH) in their nucleus at the present time and that the mass of the hosted SMBH correlates with the properties of the host bulge. Observational evidence points to the existence of a strong correlation between the mass of the central SMBH and the velocity dispersion of the host spheroid (Tremaine et al. 2002; Ferrarese & Merritt 2000, Gebhardt et al. 2003; Marconi & Hunt 2003; Haring & Rix 2004; Gultekin et al. 2009; Kormendy & Bender 2011) and possibly the host halo (Ferrarese 2002; Volonteri, Natarajan & Gultekin 2011) in nearby galaxies. These correlations plotted in Fig. 1 are strongly suggestive of co-eval growth of the SMBH and the stellar component of the host galaxy. This likely occurs via regulation of the gas supply in the galactic nucleus from the earliest times (Haehnelt, Natarajan, Rees 1998; Silk & Rees 1999; Kauffmann & Haehnelt 2000; Fabian 2002; King 2003; Thompson, Quataert & Murray 2005; Natarajan & Treister 2009; Treister et al. 2011).

Black hole growth is believed to be powered by gas accretion (Lynden-Bell 1969) and actively accreting black holes are detected as optically bright quasars. These optically bright quasars appear to exist out to the highest redshifts probed at the present time. Therefore, the mass build-up of SMBHs is likely to have commenced at extremely high

redshifts ($z > 10$). In fact, optical quasars have now been detected at $z > 6$ (e.g., Fan et al. 2004; 2006) in the Sloan Digital Sky Survey (SDSS). Hosts of high redshift quasars are often strong sources of dust emission (Omont et al. 2001; Cox et al. 2002; Carilli et al. 2002; Walter et al. 2003), suggesting that quasars were already in place in massive galaxies at a time when galaxies were undergoing vigorous star formation. Furthermore, the growth spurts of SMBHs are also seen in the X-ray waveband. The integrated emission from these X-ray quasars generates the cosmic X-ray background (XRB), and its spectrum suggests that most black-hole growth is obscured in optical wavelengths (Fabian & Iwasawa 1999; Mushotzky et al. 2000; Hasinger et al. 2001; Barger et al. 2003, 2005; Worsley et al. 2005; Treister & Urry 2006). There exist examples of obscured black-hole growth in the form of ‘Type-2’ quasars, but their detected numbers are fewer than expected from models of the XRB. However, there is tantalizing evidence from infra-red (IR) studies that dust-obscured accretion is ubiquitous (Martinez-Sansigre et al. 2005; Treister et al. 2006). Current work suggests that while SMBHs might spend most of their lifetime in an optically dim phase, the bulk of their mass growth occurs in the short-lived quasar stages (Treister et al. 2010). The assembly of BH mass in the Universe has been tracked using optical quasar activity. The current phenomenological approach to understanding the assembly of SMBHs involves optical data from both high and low redshifts. These data are used as a starting point to construct a consistent picture that fits within the larger framework of the growth and evolution of structure in the Universe (Haehnelt et al. 1998; Haiman & Loeb 1998; Kauffmann & Haehnelt 2000, 2002; Wyithe & Loeb 2002; Volonteri et al. 2003; Di Matteo et al. 2003; Volonteri, Lodato & Natarajan 2008). Optically bright quasars powered by accretion onto black holes are now detected out to redshifts of $z > 6$ when the Universe was barely 7% of its current age (Fan et al. 2004; 2006). The luminosities of these high redshift quasars imply black hole masses $M_{\text{BH}} > 10^9 M_{\odot}$.

Models that describe the growth and accretion history of supermassive black holes typically use as initial seeds the remnants derived from Population-III stars (e.g. Haiman & Loeb 1998; Haehnelt, Natarajan & Rees 1998). Assembling these large black hole masses inferred at $z \approx 6$, starting from remnants of the first generation of metal free stars has been a challenge for models. Copious growth episodes are required at early times to do so. Some suggestions to accomplish this rapid growth invoke super-Eddington accretion rates for brief periods of time (Volonteri & Rees 2005). Alternatively, it has been suggested that the formation of more massive seeds ab-initio through direct collapse of self-gravitating pre-galactic disks might offer a new channel. Such a model has been proposed by Lodato & Natarajan 2006 [LN06]. This scenario alleviates the problem of building up supermassive black hole masses to the required values by $z = 6$ without Super-Eddington accretion.

Current modeling is grounded in the framework of the standard paradigm that involves the growth of structure via gravitational amplification of small perturbations in a CDM Universe—a model that has independent validation, most recently from *Wilkinson Microwave Anisotropy Probe* (WMAP) measurements of the anisotropies in the cosmic microwave background (Dunkley et al. 2009). Structure formation is tracked over cosmic time by keeping a census of the number of collapsed dark matter halos of a given mass that form; these provide the sites for harboring black holes. The computation of the mass function of dark matter halos is done using either the Press-Schechter (Press &

Schechter 1974) or the extended Press-Schechter theory (Lacey & Cole 1993), or Monte-Carlo realizations of merger trees (Kauffmann & Haehnelt 2000; Volonteri et al. 2003; Bromley et al. 2004) or, in some cases, directly from cosmological N-body simulations (Di Matteo et al. 2003, 2005).

In particular (Volonteri et al. 2003) have presented a detailed merger-tree based scenario to trace the growth of black holes from the earliest epochs to the present day. Monte-Carlo merger trees are created for present day halos and propagated back in time to a redshift of ~ 20 . With the merging history thus determined, the initial halos at $z \sim 20$ are then populated with seed black holes which are assumed to be remnants of the first stars that form in the Universe. The masses of these so-called Population-III stars are not accurately known, however numerical simulations by various groups (Abel et al 2000; Bromm et al. 2002) suggest that they are skewed to masses of the order of a few hundred solar masses. Seeded with the end products of this first population, the merger sequence is followed and black holes are assumed to grow with every major merging episode. An accretion episode is assumed to occur as a consequence of every major merger event¹. Following the growth and mass assembly of these black holes, it is required that the model is in consonance with the observed local $M_{\text{BH}} - \sigma$ relation. The luminosity function of quasars is predicted by these models and can be compared to observations. It is found that not every halo at high redshift needs to be populated with a black hole seed in order to satisfy the observational constraints at $z = 0$. These models do not automatically reproduce the required abundance of supermassive black holes inferred to power the observed $z > 6$ SDSS quasars. In order to match the observation and produce SMBHs roughly 1 Gyr after the Big Bang, it is required that black holes undergo brief, but extremely strong growth episodes during which the accretion rate onto them is well in excess of the Eddington rate (Volonteri & Rees 2005; Begelman et al. 2006). It is the discovery and existence of this population of SMBHs powering quasars at $z > 6$ that has prompted work on alternate channels to explain their mass build-up. In order to alleviate the problem of explaining the existence of SMBHs in place by $z \sim 6$, roughly 1 Gyr after the Big Bang, we examined the possibility of using a well motivated high redshift massive seed black hole initial mass function. We populate early dark matter halos with massive black hole seeds predicted in a model proposed by Lodato & Natarajan (2006 (LN06 hereafter); 2007). This model predicts a mass function for black holes that results from the direct collapse of pre-galactic gas discs. The implications of the use of this massive seed mass function versus that of the Population-III remnants, in particular, for predictions at $z = 0$ has been studied in detail.

In this review, we present the results of this exercise and outline the evolution of high redshift seed black hole masses to late times and their observational signatures. Populating dark matter halos with initial seeds formed in this way, we follow the mass assembly of these black holes to the present time using the Monte-Carlo merger tree approach. Using this machinery we predict the black hole mass function at high redshifts and at the present time; the integrated mass density of black holes and the luminosity function of accreting black holes as a function of redshift. These predictions are made for a set of three seed models with varying black hole formation efficiency.

¹ Major mergers are defined as mergers between two dark matter halos with mass ratio between 1 and 10.

THE FORMATION OF SEED BLACK HOLES AT HIGH REDSHIFT

We focus on the main features of massive seed models here. Most aspects of the evolution and assembly history of this scenario have been explored in detail in Volonteri & Natarajan (2009) and Volonteri, Lodato & Natarajan (2008). In these models, at early times the properties of the assembling SMBH seeds are more tightly coupled to properties of the dark matter halo as their growth is driven by the merger history of halos. However, at later times, when the merger rates are low, the final mass of the SMBH is likely more tightly coupled to the small scale local baryonic distribution. The relevant host dark matter halo property at high redshifts in this picture is the spin or the angular momentum content.

In a physically motivated model for the formation of heavy SMBH seeds as described in LN06, there is a limited range of dark matter halo spins and halo masses that are viable sites for their formation. In this picture, massive seeds with $M \approx 10^5 - 10^6 M_\odot$ can form at high redshift ($z > 15$), when the intergalactic medium has not been significantly enriched by metals (Koushiappas et al. 2004; Begelman, Volonteri & Rees 2006; LN06; Lodato & Natarajan 2007). As derived in LN06, it is the development of non-axisymmetric spiral structures that drives mass infall and accumulation in a pre-galactic disc with primordial composition.

The main parameter characterizing a dark matter halo that is relevant to the fate of the gas is its spin parameter λ ($\equiv J_h E_h^{1/2} / GM_h^{5/2}$, where J_h is the total angular momentum and E_h is the binding energy). The distribution of spin parameters for dark matter halos measured in numerical simulations is well fit by a lognormal distribution in λ , with mean $\bar{\lambda} = 0.05$ and standard deviation $\sigma_\lambda = 0.5$:

$$p(\lambda) d\lambda = \frac{1}{\sqrt{2\pi}\sigma_\lambda} \exp\left[-\frac{\ln^2(\lambda/\bar{\lambda})}{2\sigma_\lambda^2}\right] \frac{d\lambda}{\lambda}, \quad (1)$$

This function has been shown to provide a good fit to the N-body results of several investigations at low redshift (e.g., Warren et al. 1992; Cole et al. 1996; Bullock et al. 2001; van den Bosch et al. 2002) as well as these high redshifts (Davis & Natarajan 2009; 2010). If the virial temperature of the halo $T_{\text{vir}} > T_{\text{gas}}$, the gas collapses and forms a rotationally supported disc. For low values of the spin parameter λ the resulting disc can be compact and dense and is subject to gravitational instabilities. This occurs when the stability parameter Q defined below approaches unity:

$$Q = \frac{c_s \kappa}{\pi G \Sigma} = \sqrt{2} \frac{c_s V_h}{\pi G \Sigma R}, \quad (2)$$

where R is the cylindrical radial coordinate, Σ is the surface mass density, c_s is the sound speed, $\kappa = \sqrt{2}V_h/R$ is the epicyclic frequency, and V_h is the circular velocity of the disc (mostly determined by the gravitational potential of the dark matter). It is also assumed that at the relevant radii ($\approx 10^2 - 10^3$ pc) the rotation curve is well described by a flat V_h profile. We consider here the earliest generations of gas discs, which are of pristine composition with no metals and therefore can cool only via hydrogen. In

thermal equilibrium, if the formation of molecular hydrogen is suppressed, these discs are expected to be nearly isothermal at a temperature of a few thousand Kelvin (here we take $T_{\text{gas}} \approx 5000\text{K}$, LN06). However, molecular hydrogen if present can cool these discs further down to temperatures of a few hundred Kelvin. The stability parameter has a critical value Q_c of the order of unity, below which the disc is unstable leading to the potential formation of a seed black hole. The actual value of Q_c essentially determines how stable the disc is, with lower Q_c 's implying more stable discs. It is well known since Toomre (1964) proposed this stability criterion, that for an infinitesimally thin disc to be stable to fragmentation, $Q_c = 1$ for axisymmetric disturbances. The exact value of Q_c under more realistic conditions is not well determined. Finite thickness effects tend to stabilize the disc (reducing Q_c), while on the other hand non-axisymmetric perturbations are in reality more unstable (enhancing Q_c). Global, three-dimensional simulations of Keplerian discs (Lodato & Rice 2004, 2005) have shown that such discs settle down in a quasi-equilibrium configuration with Q remarkably close to unity, implying that the critical value $Q_c \approx 1$. In this treatment, Q_c is taken to be a free parameter and results are computed for a range of values.

If the disc becomes unstable it develops non-axisymmetric spiral structures, which leads to an effective redistribution of angular momentum, thus feeding a growing seed black hole in the center. This process stops when the amount of mass transported to the center is enough to make the disc marginally stable. This can be computed easily from the stability criterion in eqn. (2) and from the disc properties, determined from the dark matter halo mass and angular momentum (Mo, Mao & White 1998). The mass accumulated in the center of the halo (which provides an upper limit to the SMBH seed mass) is given by:

$$M_{\text{BH}} = m_d M_{\text{halo}} \left[1 - \sqrt{\frac{8\lambda}{m_d Q_c} \left(\frac{j_d}{m_d} \right) \left(\frac{T_{\text{gas}}}{T_{\text{vir}}} \right)^{1/2}} \right] \quad (3)$$

for

$$\lambda < \lambda_{\text{max}} = m_d Q_c / 8 (m_d / j_d) (T_{\text{vir}} / T_{\text{gas}})^{1/2} \quad (4)$$

and $M_{\text{BH}} = 0$ otherwise. Here λ_{max} is the maximum halo spin parameter for which the disc is gravitationally unstable, m_d is the gas fraction that participates in the infall and Q_c is the Toomre parameter. The efficiency of SMBH formation is strongly dependent on the Toomre parameter Q_c , which sets the frequency of formation, and consequently the number density of SMBH seeds. The efficiency of the seed assembly process ceases at large halo masses, where the disc undergoes fragmentation instead. This occurs when the virial temperature exceeds a critical value T_{max} , given by:

$$\frac{T_{\text{max}}}{T_{\text{gas}}} = \left(\frac{4\alpha_c}{m_d} \frac{1}{1 + M_{\text{BH}}/m_d M_{\text{halo}}} \right)^{2/3}, \quad (5)$$

where $\alpha_c \approx 0.06$ is a dimensionless parameter measuring the critical gravitational torque above which the disc fragments. The remaining relevant parameters are assumed to have typical values: $m_d = j_d = 0.05$, $\alpha_c = 0.06$ for the $Q_c = 2$ case. The gas has a temperature $T_{\text{gas}} = 5000\text{K}$.

The process described above provides a means to transport matter from a typical scale of a few hundred parsecs down to radii of a few AU. If the halo-disc system already possesses a massive black hole seed from a previous generation, then this gas can provide a large fuel reservoir for its further growth. Note that the typical accretion rates implied by the above model are of the order of $0.01M_{\odot}/\text{yr}$, and are therefore sub-Eddington for seeds with masses of the order of $10^5M_{M_{\odot}}$ or so. If, on the other hand no black hole seed is present, then this large gas inflow can form a seed anew. The ultimate fate of the gas in this case at the smallest scales is more uncertain. One possibility, if the accretion rate is sufficiently large, has been described in detail by Begelman et al. (2006). The infalling material likely forms a quasi-star, the core of which collapses and forms a BH, while the quasi-star keeps accreting and growing in mass at a rate which would be super-Eddington for the central BH. Alternatively, the gas might form a super-massive star, which would eventually collapse and form a black hole (Shapiro & Shibata 2002). There are no quantitative estimates of how much mass would ultimately end up collapsing into the hole. Thus, the black hole seed mass estimates based on eqn. (3) should be considered as upper limits.

To give an idea of the efficiency of BH seed formation at high z within the present model, we plot in Fig. 2, the probability of forming a BH (of any mass) at $z = 18$, as a function of halo mass, for three illustrative models. It can be seen that typically up to 10% of the halos in the right mass range can form a central seed BH, the percentage rising to a maximum of $\approx 25\%$ for the high efficiency Model C (highly unstable discs), and dropping to a value of $\approx 4\%$ for the high stability and therefore low efficiency case (Model A). To summarize, every dark matter halo is characterized by its mass M (or virial temperature T_{vir}) and by its spin parameter λ . If $\lambda < \lambda_{\text{max}}$ (see eqn. 4) and $T_{\text{vir}} < T_{\text{max}}$ (eqn. 5), then a seed SMBH forms in the center. Hence SMBHs form (i) only in halos within a given range of virial temperatures, and hence, halo masses, and (ii) only within a narrow range of spin parameters, as shown in Fig. 3. High values of the spin parameter, leading most likely to disk-dominated galaxies, are strongly disfavored as seed formation sites in this model, and in models that rely on global dynamical instabilities.

THE EVOLUTION OF SEED BLACK HOLES

We follow the evolution of the MBH population resulting from the seed formation process delineated above in a Λ CDM Universe. Our approach is similar to the one described in Volonteri, Haardt & Madau (2003). We simulate the merger history of present-day halos with masses in the range $10^{11} < M < 10^{15}M_{\odot}$ starting from $z = 20$, via a Monte Carlo algorithm based on the extended Press-Schechter formalism. Every halo entering the merger tree is assigned a spin parameter drawn from the lognormal $P(\lambda)$ distribution of simulated LCDM halos. Recent work on the fate of halo spins during mergers in cosmological simulations has led to conflicting results: Vitvitska et al. (2002) suggest that the spin parameter of a halo increases after a major merger, and the angular momentum decreases after a long series of minor mergers; D’Onghia & Navarro (2007) find instead no significant correlation between spin and merger history. Given the unsettled nature of this matter, we simply assume that the spin parameter of a halo is not

modified by its merger history. When a halo enters the merger tree, we assign seed MBHs by determining if the halo meets all the requirements described in Section 2 for the formation of a central mass concentration. As we do not self-consistently trace the metal enrichment of the intergalactic medium, we consider here a sharp transition threshold, and assume that the MBH formation scenario suggested by Lodato & Natarajan ceases at $z \approx 15$. At $z > 15$, therefore, whenever a new halo appears in the merger tree (because its mass is larger than the mass resolution), or a pre-existing halo modifies its mass by a merger, we evaluate if the gaseous component meets the conditions for efficient transport of angular momentum to create a large inflow of gas which can either form a MBH seed, or feed one if already present.

The efficiency of MBH formation is strongly dependent on the critical value of the Toomre parameter Q_c . We investigate the influence of this parameter in the determination of the global evolution of the MBH population. Fig. 4 shows the number density of seeds formed in three different models with varying efficiency, with $Q_c = 1.5$ (low efficiency Model A), $Q_c = 2$ (intermediate efficiency Model B), and $Q_c = 3$ (high efficiency Model C). The solid histograms show the total mass function of seeds formed by $z = 15$ when this formation channel ceases, while the dashed histograms refer to seeds formed at a specific redshift slice at $z = 18$. The number of seeds changes by about one order of magnitude from the least efficient to the most efficient model, consistent with the probabilities shown in Fig. 2.

We assume that, after seed formation ceases, the $z < 15$ population of MBHs evolves according to a “merger driven scenario”, as described in Volonteri (2006). We assume that during major mergers MBHs accrete gas mass that scales with the fifth power of the circular velocity (or equivalently the velocity dispersion σ_c) of the host halo. We thus set the final mass of the MBH at the end of the accretion episode to 90% of the mass predicted by the $M_{\text{BH}} - \sigma_c$ correlation, assuming that the scaling does not evolve with redshift. Mergers of the BHs themselves contribute to the mass increase of the remaining 10%.

We briefly outline the merger scenario calculation here. The merger rate of halos can be estimated using eqn. (1) of Fakhouri et al. (2010), where a simple fitting formula is derived from large LCDM simulations. The merger rate per unit redshift and mass ratio (ξ) at fixed halo mass is given by:

$$\frac{dN_m}{d\xi dz}(M_h) = A \left(\frac{M_h}{10^{12} M_\odot} \right)^\alpha \xi^\beta \exp \left[\left(\frac{\xi}{\xi} \right)^\gamma \right] (1+z)^\eta. \quad (6)$$

with $A=0.0104$, $\alpha = 0.133$, $\beta = -1.995$, $\gamma = 0.263$, $\eta = 0.0993$ and $\xi = 9.72 \times 10^{-3}$. We can integrate the merger rate between $z = 0$ and say, $z = 3$, and mass ratio $\xi > 0.3$ (major mergers). This gives the number of major mergers a halo of a given mass experiences between $z = 0$ and $z = 3$. Halo mass can be translated into virial circular velocity:

$$V_c = 142 \text{ km/s} \left[\frac{M_h}{10^{12} M_\odot} \right]^{1/3} \left[\frac{\Omega_m}{\Omega_m^z} \frac{\Delta_c}{18\pi^2} \right]^{1/6} (1+z)^{1/2}, \quad (7)$$

where Δ_c is the over-density at virialization relative to the critical density. For a WMAP5 cosmology we adopt here the fitting formula $\Delta_c = 18\pi^2 + 82d - 39d^2$ (Bryan & Nor-

man 1998), where $d \equiv \Omega_m^z - 1$ is evaluated at the collapse redshift, so that $\Omega_m^z = \Omega_m(1+z)^3 / (\Omega_m(1+z)^3 + \Omega_\Lambda + \Omega_k(1+z)^2)$. It is well known that the major merger rate is an increasing function of halo mass or circular velocity, in fact we find that the expected number of mergers between $z = 0$ and $z = 3$ with mass ratio $\xi > 0.3$ is $\simeq 0.4$ for $M_h = 10^8 M_\odot$, $\simeq 0.5$ for $M_h = 10^9 M_\odot$, $\simeq 0.7$ for $M_h = 10^{10} M_\odot$, $\simeq 1.0$ for $M_h = 10^{11} M_\odot$, $\simeq 1.4$ for $M_h = 10^{12} M_\odot$, $\simeq 1.8$ for $M_h = 10^{13} M_\odot$.

In order to calculate the accreting black hole luminosity function and to follow the black hole mass growth during each accretion event, we also need to calculate the rate at which the mass, as estimated above, is accreted. This is assumed to scale with the Eddington rate for the MBH, and is based on the results of merger simulations, which heuristically track accretion onto a central MBH (Di Matteo et al. 2005; Hopkins et al. 2005; Sijacki, Springel, Di Matteo & Hernquist 2007). The time spent by a given simulated AGN at a given bolometric luminosity ² per logarithmic interval is approximated by Hopkins et al. (2005) as follows:

$$\frac{dt}{dL} = |\alpha| t_Q L^{-1} \left(\frac{L}{10^9 L_\odot} \right)^\alpha, \quad (8)$$

where $t_Q \simeq 10^9$ yr, and $\alpha = -0.95 + 0.32 \log(L_{\text{peak}}/10^{12} L_\odot)$. Here L_{peak} is the luminosity of the AGN at the peak of its activity. Hopkins et al. (2006) show that approximating L_{peak} with the Eddington luminosity of the MBH at its final mass (i.e., when it sits on the $M_{\text{BH}} - \sigma_c$ relation) compared to computing the peak luminosity with eqn. (6) above gives the same result and in fact, the difference between these 2 cases is negligible. Volonteri et al. (2006) derive the following simple differential equation to express the instantaneous accretion rate (f_{Edd} , in units of the Eddington rate) for a MBH of mass M_{BH} in a galaxy with velocity dispersion σ_c :

$$\frac{df_{\text{Edd}}(t)}{dt} = \frac{f_{\text{Edd}}^{1-\alpha}(t)}{|\alpha| t_Q} \left(\frac{\varepsilon \dot{M}_{\text{Edd}} c^2}{10^9 L_\odot} \right)^{-\alpha}, \quad (9)$$

where t is the time elapsed from the beginning of the accretion event. Solving this equation provides us the instantaneous Eddington ratio for a given MBH at a specific time, and therefore we can self-consistently grow the MBH mass. We set the Eddington ratio $f_{\text{Edd}} = 10^{-3}$ at $t = 0$. This same type of accretion is assumed to occur, at $z > 15$, following a major merger in which a MBH is not fed by disc instabilities.

We present the results of tracking the assembly history of MBHs in 2 classes of galaxies, (i) a dark matter halo with mass $2 \times 10^{12} M_\odot$ that hosts a MW type galaxy and (ii) a more massive dark matter halo, $4 \times 10^{13} M_\odot$, that hosts a massive early type (ET) galaxy (see Fig. 6). The progenitors of the MBHs in each of these host halos are tracked and plotted as measured at a given epoch. We analyze 20 realizations for each

² We convert accretion rate into luminosity assuming that the radiative efficiency equals the binding energy per unit mass of a particle in the last stable circular orbit. We associate the location of the last stable circular orbit to the spin of the MBHs, by self-consistently tracking the evolution of black hole spins throughout our calculations (Volonteri 2005). We set 20% as the maximum value of the radiative efficiency, corresponding to a spin slightly below the theoretical limit for thin disc accretion (Thorne 1974).

halo, to account for cosmic variance. Examples of growth histories are shown in Fig. 6, while statistical $M_{\text{BH}} - \sigma$ relations are shown for the two seed models.

As outlined earlier, in propagating the seeds it is assumed that accretion episodes and therefore growth spurts are triggered only by major mergers. We find that in a merger-driven scenario for MBH growth the most biased galaxies at every epoch host the most massive MBHs that are most likely already sitting on the $M_{\text{BH}} - \sigma$ relation. Lower mass MBHs (below $10^6 M_{\odot}$) are instead off the relation at $z = 4$ and even at $z = 2$. These baseline results are *independent of the seeding mechanism*. In the ‘heavy seeds’ scenario, most of the MBH seeds start out *well above* the $z = 0$ $M_{\text{BH}} - \sigma$, that is, they are ‘overmassive’ compared to the local relation. Seeds form only in halos within a narrow range of velocity dispersion ($\sigma \simeq 15 \text{ km s}^{-1}$, see equations 1 and 3, and Fig. 1). The MBH mass corresponding to $\sigma \simeq 15 \text{ km s}^{-1}$, according to the local $M_{\text{BH}} - \sigma$ relation, would be $\sim 3 \times 10^3 M_{\odot}$. The initial BH seed mass function instead peaks at $10^5 M_{\odot}$ (Lodato & Natarajan 2007). As time elapses, all halos are bound to grow in mass by mergers. The lowest mass halos, though, experience mostly minor mergers, that do not trigger accretion episodes, and hence do not grow the MBH. The evolution of these systems can be described by a shift towards the right of the $M_{\text{BH}} - \sigma$ relation: σ increases, but M_{BH} stays roughly constant. Such systems are clearly seen at $z = 1$ in Fig. 6, with $M_{\text{BH}} \sim 10^5 M_{\odot}$ and $\sigma < 100 \text{ km s}^{-1}$. Effectively, for the lowest mass halos growth of the stellar component of the galaxy and the central MBH are not coeval but rather sequential.

In the case of Population-III seeds there is initially no correlation between seed mass and halo mass or velocity dispersion. Here we have assumed that the seeds form in the mass range $125 < M_{\text{BH}} < 1000 M_{\odot}$. The initial $M_{\text{BH}} - \sigma$ relation would therefore appear as a horizontal line at $\sim 200 M_{\odot}$. In this case MBHs migrate onto the $M_{\text{BH}} - \sigma$ always from *below*, as seeds are initially ‘undermassive’ compared to the local relation. Underfed survivors of the seed epoch shift towards the right of the $M_{\text{BH}} - \sigma$ relation and lie in the lower left corner of Fig. 2, with $M_{\text{BH}} \sim 10^2 - 10^3 M_{\odot}$ and $\sigma < 100 \text{ km s}^{-1}$.

There appears to be a distinct difference between the journey of MBH seeds onto the $M_{\text{BH}} - \sigma$ relation predicted by the two seeding models considered here. The Population-III seeds start life ‘undermassive’ lying initially below the local $M_{\text{BH}} - \sigma$ and they transit up to the relation by essentially growing the MBH without significantly altering σ . In contrast, the massive seeds start off above the local $M_{\text{BH}} - \sigma$ relation, and migrate onto it by initially growing σ , after which further major mergers trigger accretion episodes and therefore growth spurts for the MBHs. When MBHs are more massive than expected compared to the $M_{\text{BH}} - \sigma$ relation, accretion is terminated very rapidly in our scheme (physically, we expect feedback to be responsible for shutting down accretion, see, e.g., Silk & Rees 1998, Fabian 2002; Natarajan & Treister 2009).

It appears that major mergers that trigger accretion episodes are what set up the relation initially at high redshift (Treister et al. 2010). Our conclusions in this regard are in agreement with those reached by alternative arguments, for instance see Peng (2007) and Robertson et al. (2006). Recent results from X-ray stacking analysis of the $z = 7 - 8$ dropouts is also consistent with the existence of self-regulation even at these early times (Treister et al. 2011). Biased peaks in the halo mass distribution, which are the sites for the formation of the largest galaxies, host the earliest massive MBHs that fall on the relation. Hence, the $M_{\text{BH}} - \sigma$ relation is established first for MBHs hosted

in the largest halos present at any time. MBHs in small galaxies lag behind, as their hosts are subject to little or no major merger activity. In many cases the MBHs remain at the original seed mass for billions of years (e.g., see Figs. 6 & 7, the $z = 1$ panel). We find that these conclusions hold irrespective of our initial seeding mechanism and the relation tightens considerably from $z = 4$ to $z = 1$, especially for MBHs hosted in halos with $\sigma > 100 \text{ km s}^{-1}$. We find that if black hole seeds are massive, $\sim 10^5 M_\odot$, the low-mass end of the $M_{\text{BH}} - \sigma$ flattens at low masses towards an asymptotic value, creating a characteristic ‘plume’. This ‘plume’ consists of ungrown seeds, that merely continue to track the peak of the seed mass function at $M_{\text{BH}} \sim 10^5 M_\odot$ down to late times. For the Population-III seed case, since the initial seed mass is very small, the plume of MBHs with $M_{\text{BH}} \sim 10^5 - 10^6 M_\odot$ in halos with $\sigma \sim 40 - 50 \text{ km s}^{-1}$ disappears.

RESULTS

The repercussions of different initial efficiencies for seed formation for the overall evolution of the MBH population stretch from high-redshift to the local Universe. Detection of gravitational waves from seeds merging at the redshift of formation (Sesana 2007) is probably one of the best ways to discriminate among formation mechanisms. On the other hand, the imprint of different formation scenarios can also be sought in observations at lower redshifts. The various seed formation scenarios have distinct consequences for the properties of the MBH population at $z = 0$ as we demonstrate below.

Given the accuracy of current observational constraints seeding models cannot be differentiated. Discrimination between the models appears predominantly at the low mass end of the present day black hole mass function which is not observationally well constrained. However, all our models predict that low surface brightness, bulgeless galaxies with large discs are least likely to be sites for the formation of massive seed black holes at high redshifts. The efficiency of seed formation at high redshifts has a direct influence on the black hole occupation fraction in galaxies at $z = 0$. This effect is more pronounced for low mass galaxies. This is the key discriminant between the models studied here and the Population-III remnant seed model as we show in detail below. We find that there exists a population of low mass galaxies that do not host nuclear black holes. Our prediction of the shape of the $M_{\text{bh}} - \sigma$ relation at the low mass end is in agreement with the recent observational determination from the census of low mass galaxies locally (Greene & Ho 2007; Kormendy & Bender 2011).

Predictions at high redshift

The luminosity function of accreting black holes

Turning to the global properties of the MBH population, as suggested by Yu & Tremaine (2002) the mass growth of the MBH population at $z < 3$ is dominated by the mass accreted during the bright epoch of quasars, thus washing out most of the imprint of initial conditions. This is evident when we compute the luminosity function of AGN.

Clearly the detailed shape of the predicted luminosity function depends most strongly on the accretion prescription used. With our assumption that the gas mass accreted during each merger episode is proportional to V_c^5 , we find that distinguishing between the various seed models is difficult. As shown in Fig. 4, all 3 models reproduce the bright end of the observed bolometric LF (Hopkins et al. 2007) at higher redshifts (marked as the solid curve in all the panels), and predict a fairly steep faint end that is as yet undetected. All models fare less well at low redshift, shown in particular at $z = 0.5$. This could be due to the fact that we have used a single accretion prescription to model growth through epochs. On the other hand, the decline in the available gas budget at low redshifts (since the bulk of the gas has been consumed by this epoch by star formation activity) likely changes the radiative efficiency of these systems. Besides, observations suggest a sharp decline in the number of actively accreting black holes at low redshifts across wavelengths, produced most probably due to changes in the accretion flow as a result of change in the geometry of the nuclear regions of galaxies. In fact, all 3 of our models under-predict the slope at the faint end. There are three other effects that could cause this flattening of the LF at the faint end at low redshift for our models: (i) not having taken into account the fate of on-going merging and the fate of satellite galaxies; (ii) the number of realizations generated and tracked is insufficient for statistics, as evidenced by the systematically larger error-bars and (iii) more importantly, it is unclear if merger-driven accretion is indeed the trigger of BH fueling in the low redshift universe. We note that the 3 massive seed models and Population-III seed model cannot be discriminated by the LF at high redshifts. Models B and C are also in agreement viz-a-viz the predicted BH mass function at $z = 6$, even assuming a very high radiative efficiency (up to 20%), while Model A might need less severe assumptions, in particular for BH masses larger than $10^7 M_\odot$.

Low redshift predictions

Supermassive black holes in dwarf galaxies

Obviously, a higher density of MBH seeds implies a more ubiquitous population of MBHs at later times, which can produce observational signatures in statistical samples. More subtly, the formation of seeds in a Λ CDM scenario follows the cosmological bias. As a consequence, the progenitors of massive galaxies have a higher probability of hosting MBH seeds (cfr. Madau & Rees 2001). In the case of low-bias systems, such as isolated dwarf galaxies, very few of the high- z progenitors have the deep potential wells needed for gas retention and cooling, a prerequisite for MBH formation. In the lowest efficiency massive seed Model A, for example, a galaxy needs of order 25 massive progenitors (mass above $\sim 10^7 M_\odot$) to ensure a high probability of seeding within the merger tree. In the massive seed Model C, instead, the requirement drops to 4 massive progenitors, increasing the probability of MBH formation in lower bias halos.

The signature of the efficiency of the formation of MBH seeds will consequently be stronger in isolated dwarf galaxies. Fig. 5 (bottom panel) shows a comparison between the observed $M_{\text{BH}} - \sigma$ relation and the one predicted by our models (shown with circles),

and in particular, from left to right, the three models based on the LN06 and Lodato & Natarajan (2007) seed masses with $Q_c = 1.5, 2$ and 3 , and a fourth model based on lower-mass Population-III star seeds. The upper panel of Fig. 5 shows the fraction of galaxies that **do not** host any massive black holes for different velocity dispersion bins. This shows that the fraction of galaxies without a MBH increases with decreasing halo masses at $z = 0$. A larger fraction of low mass halos are devoid of central black holes for lower seed formation efficiencies. Note that this is one of the key discriminants between our models and those seeded with Population-III remnants. As shown in Fig. 3, there are practically no galaxies without central BHs for the Population-III seeds. We can therefore make quantitative predictions for the local occupation fraction of MBHs. Our massive seeding Model A predicts that below $\sigma_c \approx 60 \text{ km s}^{-1}$ the probability of a galaxy hosting a MBH is negligible. With increasing MBH formation efficiencies, the minimum mass for a galaxy that hosts a MBH decreases, and it drops below our simulation limits for Model C. On the other hand, models based on lower mass Population-III star remnant seeds, predict that massive black holes might be present even in low mass galaxies. These predictions appear to be consistent with recent observations of low mass galaxies (Kormendy & Bender 2011).

Although there are degeneracies in our modeling (e.g., between the minimum redshift for BH formation and instability criterion), the BH occupation fraction, and the masses of the BHs in dwarf galaxies are the key diagnostics. An additional caveat worth mentioning is the possibility that a galaxy is devoid of a central MBH because of dynamical ejections (due to either the gravitational recoil or three-body scattering). The signatures of such dynamical interactions should be more prominent in dwarf galaxies, but ejected MBHs would leave observational signatures on their hosts (Gültekin et al. in prep.). On top of that, Schnittman (2007) and Volonteri, Lodato & Natarajan (2007) agree in considering the recoil a minor correction to the overall distribution of the MBH population at low redshift (cfr. Fig. 4 in Volonteri 2007). Additionally, as MBH seed formation requires halos with low angular momentum (low spin parameter), we envisage that low surface brightness, bulge-less galaxies with high spin parameters (i.e. large discs) are systems where MBH seed formation is less probable. Furthermore, bulgeless galaxies are believed to preferentially have quieter merger histories and are unlikely to have experienced major mergers, which could have brought in a MBH from a companion galaxy. This prediction of the massive seeding models appears to be in consonance with recent observational studies by Kormendy & Bender (2011).

Seed signatures for the detection of gravitational waves

An alternative to AGN observations in electromagnetic bands is the detection of MBHs via gravitational radiation, that would be detectable by proposed future missions like *LISA*. The merger rate of MBHs in our models, and the detectability of binaries has been discussed in Sesana et al. (2007), where the impact of different ‘seed’ formation scenarios was taken into account. Since the focus here is on high-redshift objects, we assume that merging is driven by dynamical friction, which has been shown to efficiently drive the MBHs in the central regions of the newly formed galaxy when the mass

ratio of the satellite halo to the main halo is sufficiently large, $> 1 : 10$ and galaxies are gas-rich (Callegari et al. 2008). The available simulations (Armitage & Natarajan 2002; Escala et al. 2004; Dotti et al. 2006; Mayer et al. 2006) show that the binary can shrink to about parsec or slightly subparsec scale by dynamical friction against gas. We refer the reader to Sesana et al. (2007) and Sesana et al. (2005) for a detailed discussion of how we model the gravitational wave emission and the expected event rate. Detection of gravitational radiation provides accurate measurements of the mass of the components of MBH binaries prior to merger, and the mass of the single merger remnant. Additionally, the mass of ‘single’ MBHs can be determined by the inspiral of an extreme or intermediate mass-ratio compact object (EMRI/IMRI, Miller 2005).

When we track the merging population, we find that MBH-MBH mergers also preferentially sample the region of space where MBHs lie on the $M_{\text{BH}} - \sigma$ relation. This is once again a consequence of halo bias. Both channels for seed formation that we investigate here require deep potential wells for gas retention and cooling as a prerequisite for MBH formation. Halos where massive seeds can form are typically $3.5-4 \sigma$ peaks of the density fluctuation field at $z > 15$, (the host halos in the direct collapse model are slightly more biased than in the Population-III remnant case). MBH seeding is therefore infrequent, MBHs are rare and as a consequence MBH-MBH mergers are events that typically involve only the most biased halos at any time.

In typical mergers we find that the higher mass black hole in the binary tends to sit on or near the expected $M_{\text{BH}} - \sigma$ relation for the host (which corresponds to the newly formed galaxy after the merger). The mass of the secondary generally provides clues to the dynamics of the merger, rather than to the $M_{\text{BH}} - \sigma$ relation, since at the time of the merger any information that we can gather on the host (via electromagnetic observations) will not provide details on the two original galaxies. For instance the mass ratio of the merging MBHs encodes how efficiently minor mergers can deliver MBHs to the centre of a galaxy in order to form a bound binary.

Hidden black holes

One key finding is the prediction of the existence of a large population of hidden (as in undetectable as AGN or as merging BHs via gravitational radiation) MBHs at all redshifts. There are two main contributors to the population of hidden MBHs: MBHs in the *nuclei* of low-mass galaxies ($\sigma \sim 20 - 50 \text{km s}^{-1}$), and satellite/wandering MBHs. ‘Hidden’ nuclear MBHs have not experienced appreciable growth in mass and formed in low mass halos with quiet merging histories. A potential observational signature of the massive seed scenario is the existence of a ‘plume’ of overmassive MBHs in the *nuclei* of halos with $\sigma \sim 20 - 50 \text{km s}^{-1}$. The only way to detect MBHs in the plume would be as IMRI/EMRI (intermediate or extreme mass ratio inspiral) events, or via measurement of stellar velocity dispersions and modelling as in the local universe (for example Magorrian et al. 1998). Approaching $z = 0$, the under-fed part of this population likely merges into more massive galaxies.

Satellite and wandering MBHs would instead be off-centre systems, orbiting in the potential of comparatively massive hosts. Semantically we distinguish here between

MBHs that are infalling into a galaxy for the very first time, following a galaxy merger (satellite MBHs) and those that are merely displaced from the center due to gravitational recoil (wandering MBHs). Some of the *satellite* MBHs will merge with the central MBH in the primary galaxy, and such merging does not significantly alter the position of the already massive primary hole which sits on the $M_{\text{BH}} - \sigma$ relation to start with.

The MBH population in our series of simulations of the massive ET halo is shown in Fig. 6, for $z = 1$. Here we dissect the MBH population into its components. Satellite/wandering MBHs are found *below* the $M_{\text{BH}} - \sigma$ correlation as expected (shown as open circles, at the σ of the host halo). Luminous AGNs are preferentially found on the $M_{\text{BH}} - \sigma$ relation (squares). We note the existence of a sub-population of satellite AGNs, that is, satellite MBHs which are actively accreting. For every pair of coalescing MBHs (triangles), one typically sits on the $M_{\text{BH}} - \sigma$ relation, while the companion tends to be less massive, hence, when they merge, the remnant finds itself in the right spot on the $M_{\text{BH}} - \sigma$ relation (solid circles).

Comoving mass density of black holes

Since during the quasar epoch MBHs increase their mass by a large factor, signatures of the seed formation mechanisms are likely more evident at *earlier epochs*. We compare in Fig. 8 the integrated comoving mass density in MBHs to the expectations from Sołtan-type arguments, assuming that quasars are powered by radiatively efficient flows (for details, see Yu & Tremaine 2002; Elvis, Risaliti & Zamorini 2002; Marconi et al. 2004). While during and after the quasar epoch the mass densities in models A, B, and C differ by less than a factor of 2, at $z > 3$ the differences are more pronounced.

A very efficient seed MBH formation scenario can lead to a very large BH density at high redshifts. For instance, in the highest efficiency Model C with $Q_c = 3$, the integrated MBH density at $z = 10$ is already $\sim 25\%$ of the density at $z = 0$. The plateau at $z > 6$ is due to our choice of scaling the accreted mass with the $z = 0$ $M_{\text{bh}} - \sigma$ relation. In our models we let MBHs accrete mass that scales with the fifth power of the circular velocity of the halo, the accreted mass is a small fraction of the MBH mass (see the discussion in Marulli et al. 2006), and the overall growth remains small, as long as the mass of the seed is larger than the accreted mass, which, for our assumed scaling, happens whenever the mass of the halo is below a few times $10^{10} M_{\odot}$. The comoving mass density, an integral constraint, is reasonably well determined out to $z = 3$ but is poorly known at higher redshifts. All models appear to be satisfactory and consistent with current observational limits (shown as the shaded area).

Black hole mass function at $z = 0$

One of the key diagnostics is the comparison of the measured and predicted BH mass function at $z = 0$ for our 3 models. In Fig. 9, we show (from left to right, respectively) the mass function predicted by models A, B, C and Population-III remnant seeds compared to that obtained from measurements. The histograms show the mass function obtained

with our models (where the upper histogram includes all the black holes while the lower one only includes black holes found in central galaxies of halos in the merger-tree approach). The two lines are two different estimates of the observed black hole mass function. In the upper one, the measured velocity dispersion function for nearby late and early-type galaxies from the SDSS survey (Bernardi et al. 2003; Sheth et al. 2003) has been convolved with the measured $M_{\text{BH}} - \sigma$ relation. We note here that the scatter in the $M_{\text{bh}} - \sigma$ relation is not explicitly included in this treatment, however the inclusion of the scatter is likely to preferentially affect the high mass end of the BHMF, which provides stronger constraints on the accretion histories rather than the seed masses. It has been argued by Tundo et al. (2007); Bernardi et al. (2007) and Lauer et al. (2007) that the BH mass function differs if the bulge mass is used instead of the velocity dispersion in relating the BH mass to the host galaxy. Since our models do not trace the formation and growth of stellar bulges in detail, we are restricted to using the velocity dispersion in our analysis.

The lower dashed curve is an alternate theoretical estimate of the BH mass function derived using the Press-Schechter formalism from Jenkins et al. (2001) in conjunction with the observed $M_{\text{BH}} - \sigma$ relation. Selecting only the central galaxies of halos in the merger-tree approach adopted here (lower histograms) is shown to be equivalent to this analytical estimate, and this is clearly borne out in the plot. When we include black holes in satellite galaxies (upper histograms, cfr. the discussion in Volonteri, Haardt & Madau 2003) the predicted mass function moves towards the estimate based on SDSS galaxies. The higher efficiency models clearly produce more BHs. At higher redshifts, for instance at $z = 6$, the mass functions of active MBHs predicted by all models are in very good agreements in particular for BH masses larger than $10^6 M_{\odot}$, as it is the growth by accretion that dominates the evolution of the population. At the highest mass end ($> 10^9 M_{\odot}$) Model A lags behind models B and C, although we stress once again that our assumptions for the accretion process are very conservative.

The *relative* differences between Models A, B, and C at the low-mass end of the mass function, however, are genuinely related to the MBH seeding mechanism (see also Figs. 2 & 4). In Model A, simply, fewer galaxies host a MBH, hence reducing the overall number density of black holes. Although our simplified treatment does not allow robust quantitative predictions, the presence of a "bump" at $z = 0$ in the MBH mass function at the characteristic mass that marks the peak of the seed mass function (cfr. Fig. 4) is a sign of highly efficient formation of massive seeds (i.e., much larger mass with respect, for instance, Population-III remnants). The higher the efficiency of seed formation, the more pronounced is the bump (note that the bump is most prominent for Model C). Since current measurements of MBH masses extend barely down to $M_{\text{bh}} \sim 10^6 M_{\odot}$, this feature cannot be observationally tested with present data but future campaigns, with the Giant Magellan Telescope or JWST, are likely to extend the mass function measurements to much lower black hole masses.

CONCLUSIONS

In this review, we outline massive black hole seed formation models and focus on the consequences on their assembly history as a function of cosmic epoch. While the errors

on mass determinations of local black holes are large at the present time, definite trends with host galaxy properties are observed. The tightest correlation appears to be between the BH mass and the velocity dispersion of the host spheroid. Starting with the ab-initio black hole seed mass function computed in the context of direct formation of central objects from the collapse of pre-galactic discs in high redshift halos, we follow the assembly history to late times using a Monte-Carlo merger tree approach. Key to our calculation of the evolution and build-up of mass is the prescription that we adopt for determining the precise mass gain during a merger. Motivated by the phenomenological observation of $M_{\text{BH}} \propto V_c^5$, we assume that this proportionality carries over to the gas mass accreted in each step. With these prescriptions, a range of predictions can be made for the mass function of black holes at high and low z , and the integrated mass density of black holes, all of which are observationally determined. We evolve 3 models, designated Model A, B and C which correspond to increasing efficiencies respectively for the formation of seeds at high redshift. These models are compared to one in which the seeds are remnants of Population-III stars.

It is important to note here that one major uncertainty prevents us from making more concrete predictions: the unknown metal enrichment history of the Universe. Key to the implementation of our models is the choice of redshift at which massive seed formation is quenched. The direct seed formation channel described here ceases to operate once the Universe has been enriched by metals that have been synthesized after the first generation of stars have gone supernova. Once metals are available in the Inter-Galactic Medium gas cooling is much more efficient and hydrogen in either atomic or molecular form is no longer the key player. In this work, we have assumed this transition redshift to be $z = 15$. The efficiency of MBH formation and the transition redshift are somewhat degenerate (e.g., a model with $Q = 1.5$ and enrichment redshift $z = 12$ is halfway between Model A and Model B); if other constraints on this redshift were available we could considerably tighten our predictions.

Below we list our predictions and compare how they fare with current observations. The models investigated here clearly differ notably in predictions at the low mass end of the black hole mass function. With future observational sensitivity in this domain, these models can be distinguished.

1. Occupation fraction at $z = 0$: Our model for the formation of relatively high-mass black hole seeds in high- z halos has direct influence on the black hole occupation fraction in galaxies at $z = 0$. All our models predict that low surface brightness, bulge-less galaxies with high spin parameters (i.e. large discs) are systems where MBH formation is least probable. We find that a significant fraction of low-mass galaxies might not host a nuclear black hole. This is in very good agreement with the shape of the $M_{\text{bh}} - \sigma$ relation determined recently from an observational census (an HST ACS survey) of low mass galaxies in the Virgo cluster reported by Ferrarese et al. (2006). While current data in the low mass regime is scant (Barth 2004; Greene & Ho 2007; Kormendy & Bender 2010), future instruments and surveys are likely to probe this region of parameter space with significantly higher sensitivity.
2. High mass end of the local SMBH mass function: While the models studied here (with different black hole seed formation efficiency) are distinguishable at the

low mass end of the BH mass function, at the high mass end the effect of initial seeds appears to be sub-dominant. These models cannot be easily distinguished by observations at $z \sim 3$.

One of the key caveats of our picture is that it is unclear if the differences produced by different seed models on observables at $z = 0$ might be compensated or masked by BH fueling modes at earlier epochs. There could be other channels for BH growth that dominate at low redshifts like minor mergers, dynamical instabilities, accretion of molecular clouds, tidal disruption of stars. The decreased importance of the merger driven scenario is patent from observations of low-redshift AGN, which are for the large majority hosted by undisturbed galaxies (e.g. Pierce et al. 2007 and references therein) in low-density environments. However, the feasibility and efficiency of some alternative channels are still to be proven (for example the efficiency of feeding from large scale instabilities see discussion in King & Pringle 2007; Shlosman 1989; Goodman 2003; Collin 1999). In any event, while these additional channels for BH *growth* can modify the detailed shape of the mass function of MBHs, or of the luminosity function of quasars, they will not create new MBHs. The occupation fraction of MBHs (see Fig. 5) is therefore largely *independent* of the accretion mechanism and a true signature of the formation process.

To date, most theoretical models for the evolution of MBHs in galaxies do not include *how* MBHs form. Our work offers a first analysis of the observational signatures of massive black hole formation mechanisms in the low redshift universe, complementary to the investigation by Sesana et al. (2007), where the focus was on detection of seeds at the very early times where they form, via gravitational waves emitted during MBH mergers. We focus here on possible dynamical signatures that forming massive black hole seeds imprint on the local Universe. Obviously, the signatures of seed formation mechanisms will be far more clear if considered jointly with the evolution of the spheroids that they host. The mass, and especially the frequency, of the forming MBH seeds is a necessary input when investigating how the feedback from accretion onto MBHs influences the host galaxy, and is generally introduced in numerical models using extremely simplified, *ad hoc* prescriptions (e.g., Springel et al. 2005; Di Matteo, Springel & Hernquist 2005; Hopkins et al. 2006; Croton et al. 2005; Cattaneo et al 2006; Bower et al. 2006). Adopting more detailed models for black hole seed formation, as outlined here, can in principle strongly affect such results. Incorporating sensible assumptions for the masses, and frequency of MBH seeds in models of galaxy formation is necessary if we want to understand the symbiotic growth of MBHs and their hosts. Much work remains to be done in order to obtain a deeper understanding of the accretion history of BHs over cosmic time.

ACKNOWLEDGMENTS

PN would like to acknowledge her collaborators Marta Volonteri and Giuseppe Lodato with whom most of this work was done. She would also to thank the John Simon Guggenheim Foundation for support via a Guggenheim fellowship and the Institute for Theory and Computation at Harvard University for hosting her.

REFERENCES

- . Abel, T., Bryan, G., & Norman, M., 2000, ApJ, 540, 39
- . Barger, A. J., et al., 2003, AJ, 126, 632
- . Barger, A. J., et al., 2005, AJ, 129, 578
- . Barth, A., Ho, L., Routledge, R., & Sargent, W., 2004, 607, 90
- . Begelman, M. C., Volonteri, M., & Rees, M. J. 2006, MNRAS, 370, 289
- . Bernardi, M., et al., 2003, AJ, 125, 1882
- . Bernardi, M., et al., 2007, ApJ, 660, 267
- . Bower, R., et al., 2006, MNRAS, 370, 645
- . Bromm, V., Coppi, P., & Larson, R., 2002, ApJ, 564, 23
- . Bullock, J. S., Dekel, A., Kolatt, T. S., Kravtsov, A. V., Klypin, A. A., Porciani, C., & Primack, J. R. 2001, ApJ, 555, 240
- . Carilli, C. L., et al. 2002, AJ, 123, 1838
- . Cattaneo, A., Dekel, A., Devriendt, J., Guiderdoni, B., & Blaizot, J. 2006, MNRAS, 370, 1651
- . Collin, S., & Zahn, J.-P. 1999, A&A, 344, 433
- . Croton, D. J., et al. 2005, MNRAS, 356, 1155
- . Cox, P., et al. 2002, A&A, 387, 406
- . Davis, A., & Natarajan, P., 2009, MNRAS, 393, 1498
- . Davis, A., & Natarajan, P., 2010, MNRAS, 407, 691
- . Di Matteo, T., Springel, V., & Hernquist, L. 2005, Nature, 433, 604
- . Di Matteo, T., Croft, R. A. C., Springel, V., & Hernquist, L. 2003, ApJ, 593, 56
- . D'Onghia, E., & Navarro, J. F. 2007, MNRAS, 380, L58
- . Dotti, M., Volonteri, M., Perego, A., Colpi, M., Ruszkowski, M., & Haardt, F. 2010, MNRAS, 402, 682
- . Dunkley, J., et al., ApJS, 180, 306
- . Elvis, M., Risaliti, G., & Zamorani, G. 2002, ApJ, 565, L75
- . Fabian, A. C. 1999, MNRAS, 308, L39
- . Fabian A. C., 2002, ASPC, 258, 185
- . Fakhouri, O., Ma, C., & Boylan-Kolchin, M. 2010, MNRAS, 406, 2267
- . Ferrarese L., 2002, ApJ, 572, 90
- . Ferrarese L., & Merritt D., 2000, ApJ, 539, L9
- . Gebhardt K., et al., 2003, ApJ, 583, 92
- . Goodman, J. 2003, MNRAS, 339, 937
- . Greene, J. E., & Ho, L. C. 2007, ApJ, 670, 92
- . Gültekin, K., Richstone, D. O., Gebhardt, K., Lauer, T. R., Tremaine, S., Aller, M. C., Bender, R., Dressler, A., Faber, S. M., Filippenko, A. V., Green, R., Ho, L. C., Kormendy, J., Magorrian, J., Pinkney, J., & Siopis, C. 2009, ApJ, 698, 198
- . Haehnelt M., Natarajan P., Rees M. J., 1998, MNRAS, 300, 817
- . Haiman, Z., & Loeb, A. 1998, ApJ, 503, 505
- . Haring N., & Rix H. W., 2004, ApJ, 604, L89
- . Hasinger, G., et al. 2001, A&A, 365, L45
- . Hogg, D. W., Bovy, J., & Lang, D. 2010, ArXiv e-prints
- . Hopkins, P. F., Hernquist, L., Cox, T. J., Di Matteo, T., Robertson, B., & Springel, V. 2005, ApJ, 632, 81
- . Hopkins, P. F., Hernquist, L., Cox, T. J., Di Matteo, T., Robertson, B., & Springel, V. 2006, ApJS, 163, 1
- . Hopkins, P. F., Richards, G. T., & Hernquist, L. 2007, ApJ, 654, 731
- . Jenkins, A., Frenk, C. S., White, S. D. M., Colberg, J. M., Cole, S., Evrard, A. E., Couchman, H. M. P., & Yoshida, N. 2001, MNRAS, 321, 372
- . Kauffmann, G., & Haehnelt, M. G. 2002, MNRAS, 332, 529
- . Kauffmann G., & Haehnelt M., 2000, MNRAS, 311, 576
- . King A., 2003, ApJ, 596, L27
- . King, A. R., & Pringle, J. E. 2007, MNRAS, 377, L25
- . Kormendy, J. & Bender, R. 2011, Nature, 469, 377
- . Kormendy, J., Bender, R., & Cornell, M. E. 2011, Nature, 469, 374
- . Koushiappas, S. M., Bullock, J. S., & Dekel, A. 2004, MNRAS, 354, 292

- . Lacey, C., & Cole, S. 1993, MNRAS, 262, 627
- . Lauer, T. R., et al. 2007, ApJ, 662, 808
- . Lodato, G. & Natarajan, P. 2006, MNRAS, 371, 1813
- . Lodato, G., & Natarajan, P., 2007, MNRAS, 377, L64
- . Lynden-Bell, D. 1969, Nature, 223, 690
- . Madau, P., & Rees, M. J. 2001, ApJ, 551, L27
- . Marconi A., & Hunt L., 2003, ApJ, 598, L21
- . Marulli, F., Crociani, D., Volonteri, M., Branchini, E., & Moscardini, L. 2006, MNRAS, 368, 1269
- . Martínez-Sansigre, A., Rawlings, S., Lacy, M., Fadda, D., Marleau, F. R., Simpson, C., Willott, C. J., & Jarvis, M. J. 2005, Nature, 436, 666
- . Mo, H. J., Mao, S., & White, S. D. M. 1998, MNRAS, 295, 319
- . Natarajan P., & Treister E., 2009, MNRAS, 393, 838
- . Omont, A., Cox, P., Bertoldi, F., McMahon, R. G., Carilli, C., & Isaak, K. G. 2001, A&A, 374, 371
- . Peng, C. Y., 2007, ApJ, 671, 1098
- . Pierce, C. M., et al. 2007, ApJ, 660, L19
- . Press, W. H., & Schechter, P. 1974, ApJ, 187, 425
- . Rice W. K. M., Lodato G., Armitage P. J., 2005, MNRAS, 364, L56
- . Robertson, B., Bullock, J. S., Cox, T. J., Di Matteo, T., Hernquist, L., Springel, V., & Yoshida, N. 2006, ApJ, 645, 986
- . Schnittman, J. D. 2007, ApJ, 667, L133
- . Shlosman, I., Frank, J., & Begelman, M. C. 1989, Nature, 338, 45
- . Sesana, A., Volonteri, M., & Haardt, F. 2007, MNRAS, 377, 1711
- . Sheth, R. K., et al. 2003, ApJ, 594, 225
- . Shapiro, S. L., & Shibata, M. 2002, ApJ, 577, 904
- . Sijacki, D., Springel, V., Di Matteo, T., & Hernquist, L. 2007, MNRAS, 380, 877
- . Silk, J. & Rees, M. J. 1998, A&A, 331, L1
- . Springel, V., et al. 2005, Nature, 435, 629
- . Thompson T., Murray J., & Quatter E., 2005, ApJ, 630, 161
- . Thorne, K. S. 1974, ApJ, 191, 507
- . Treister, E., et al., 2006, ApJ, 640, 603
- . Treister E., & Urry, M., 2006, ApJ, 652, L79
- . Treister, E., Natarajan, P., et al., 2010, Science, 328, 600
- . Treister, E., Volonteri, M., Schawinski, K., Natarajan, P., & Gawiser, E., 2011, submitted to Nature
- . Tremaine S., et al, 2002, ApJ, 574, 740
- . Tundo, E., Bernardi, M., Hyde, J. B., Sheth, R. K., & Pizzella, A. 2007, ApJ, 663, 53
- . van den Bosch, F. C., Abel, T., Croft, R. A. C., Hernquist, L., & White, S. D. M. 2002, ApJ, 576, 21
- . van Meter, J. R., Miller, M. C., Baker, J. G., Boggs, W. D., & Kelly, B. J. 2010, ApJ, 719, 1427
- . Vitvitska, M., Klypin, A. A., Kravtsov, A. V., Wechsler, R. H., Primack, J. R., & Bullock, J. S. 2002, ApJ, 581, 799
- . Volonteri, M., Gültekin, K., & Dotti, M. 2010, MNRAS, 404, 2143
- . Volonteri, M., Lodato, G., & Natarajan, P. 2008, MNRAS, 383, 1079
- . Volonteri, M. & Natarajan, P. 2009, MNRAS, 400, 1911
- . Walter, F., et al. 2003, Nature, 424, 406
- . Warren, M. S., Quinn, P. J., Salmon, J. K., & Zurek, W. H. 1992, ApJ, 399, 405
- . Worsley, M. A., et al. 2005, MNRAS, 357, 1281
- . Wyithe, J. S. B., & Loeb, A. 2002, ApJ, 581, 886
- . Yu, Q., & Tremaine, S. 2002, MNRAS, 335, 965

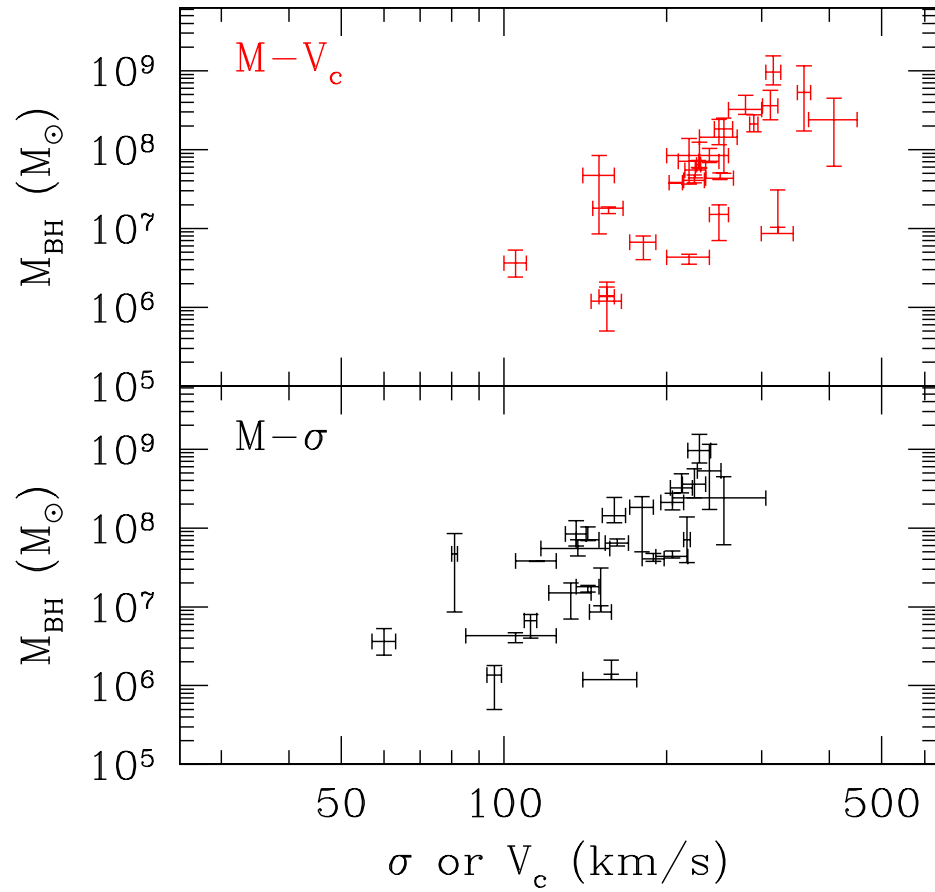


FIGURE 1. Top panel: $M_{\text{BH}} - V_c$ relation for the 25 galaxies from recently published Table 1 of Kormendy et al. (2011). Bottom panel: The $M_{\text{BH}} - \sigma$ relation from Kormendy's table. We note that M33 is omitted from this data set.

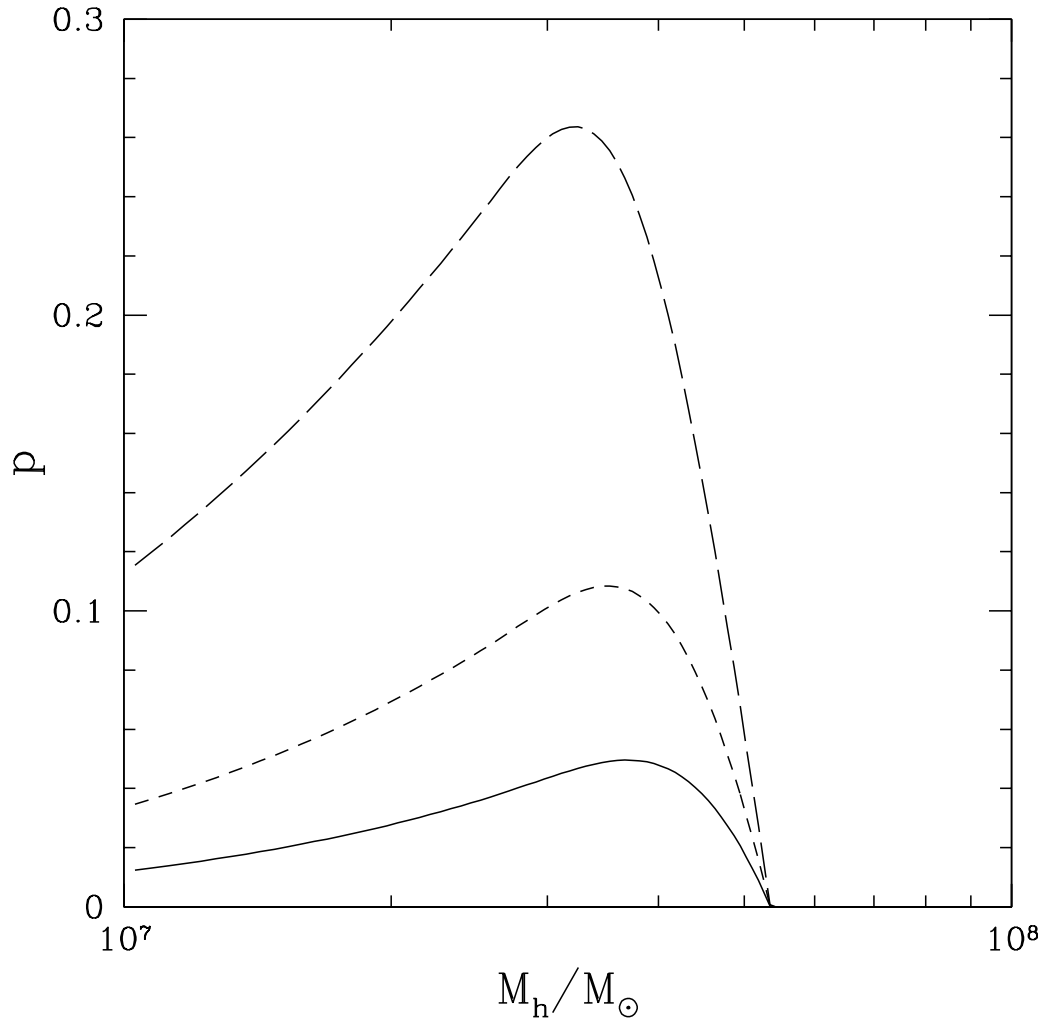


FIGURE 2. The probability of hosting a BH seed of any mass at $z = 18$ as a function of dark matter halo mass. The three curves refer to $Q_c = 1.5$ (low efficiency case Model A, solid line), $Q_c = 2$ (intermediate efficiency case Model B, short-dashed line) and $Q_c = 3$ (high efficiency case Model C, long-dashed line).

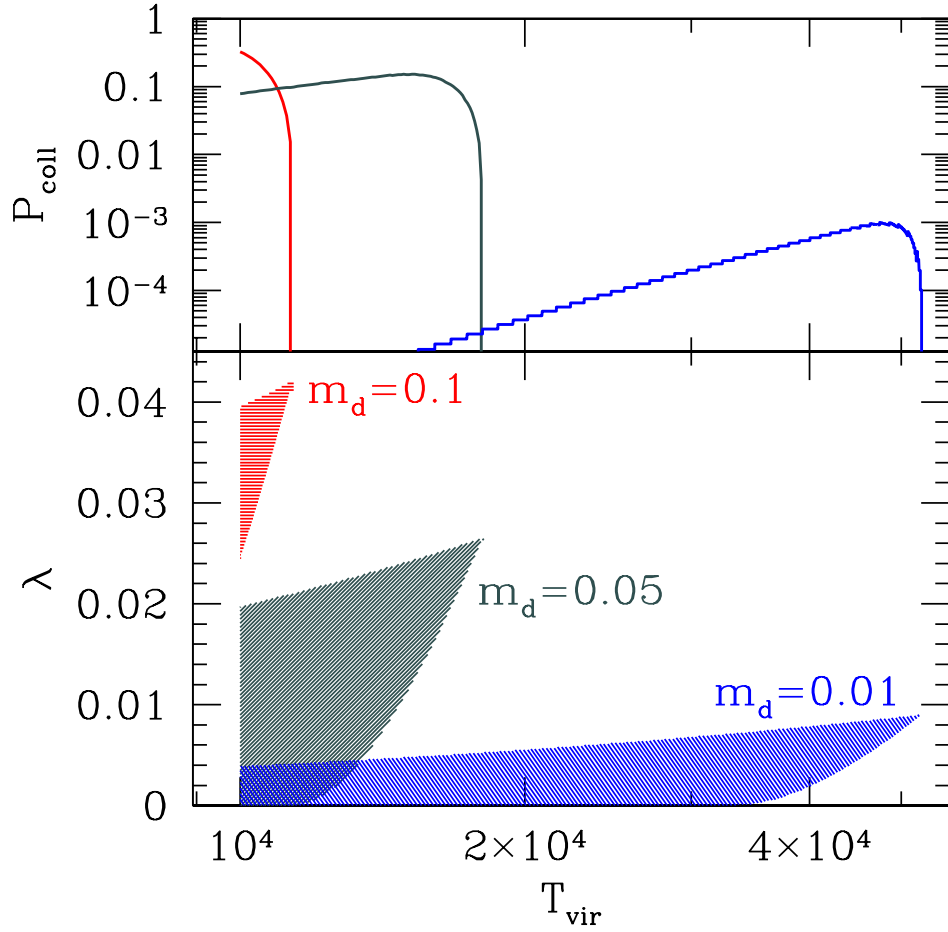


FIGURE 3. Parameter space (virial temperature, spin parameter) for SMBH formation. Halos with $T_{\text{vir}} > 10^4$ K at $z = 15$ are picked to participate in the infall (m_d). The shaded areas in the bottom panel show the range of virial temperatures and spin parameters where discs are Toomre unstable and the joint conditions, $\lambda < \lambda_{\text{max}}$ (eqn. 4) and $T_{\text{vir}} < T_{\text{max}}$ (eqn. (5)), showing the minimum spin parameter, λ_{min} value below which the disc is globally prone to fragmentation) are fulfilled. The top panel shows the probability of SMBH formation and is obtained, by integrating the lognormal distribution of spin parameters between λ_{min} and λ_{max} .

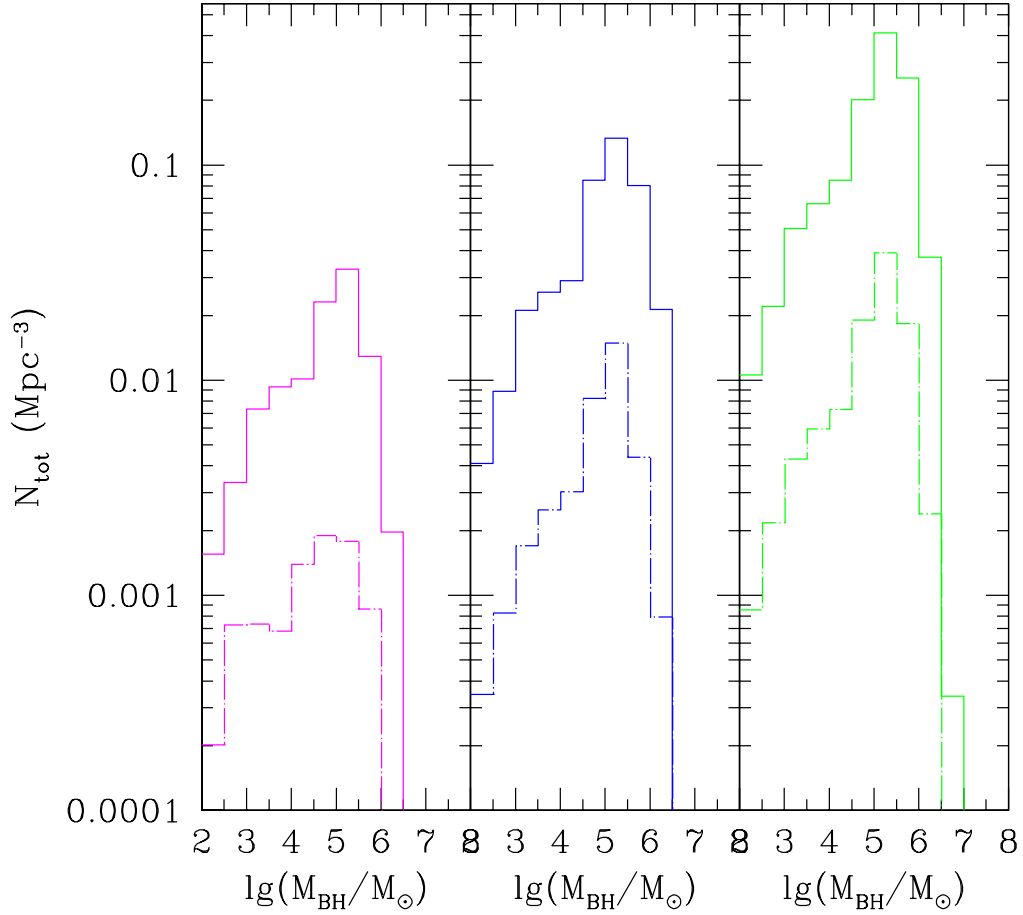


FIGURE 4. Mass function of MBH seeds in the three Q-models of that differ in seed formation efficiency. Left panel: $Q_c = 1.5$ (the least efficient Model A), middle panel: $Q_c = 2$ (intermediate efficiency Model B), right panel: $Q_c = 3$ (highly efficient Model C). Seeds form at $z > 15$ and this channel ceases at $z = 15$. The solid histograms show the total mass function of seeds formed by $z = 15$, while the dashed histograms refer to seeds formed at a specific redshift, $z = 18$.

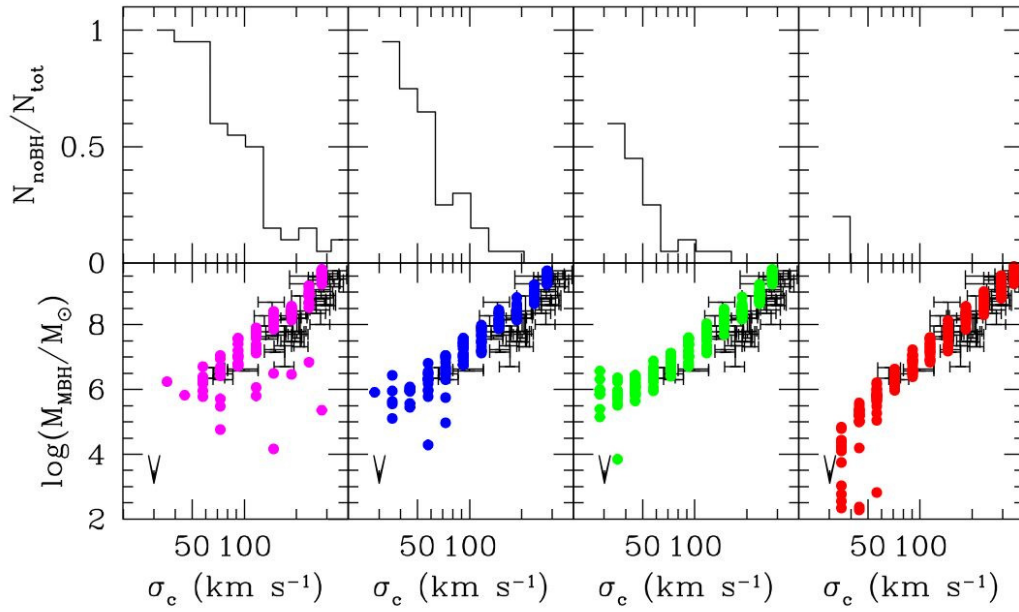


FIGURE 5. The M_{bh} –velocity dispersion (σ_c) relation at $z = 0$. Every circle represents the central MBH in a halo of given σ_c . Observational data are marked by their quoted errorbars, both in σ_c , and in M_{bh} (Tremaine et al. 2002). Left to right panels: $Q_c = 1.5$, $Q_c = 2$, $Q_c = 3$, Population-III remnant seeds. *Top panels:* fraction of galaxies at a given velocity dispersion which **do not** host a central MBH.

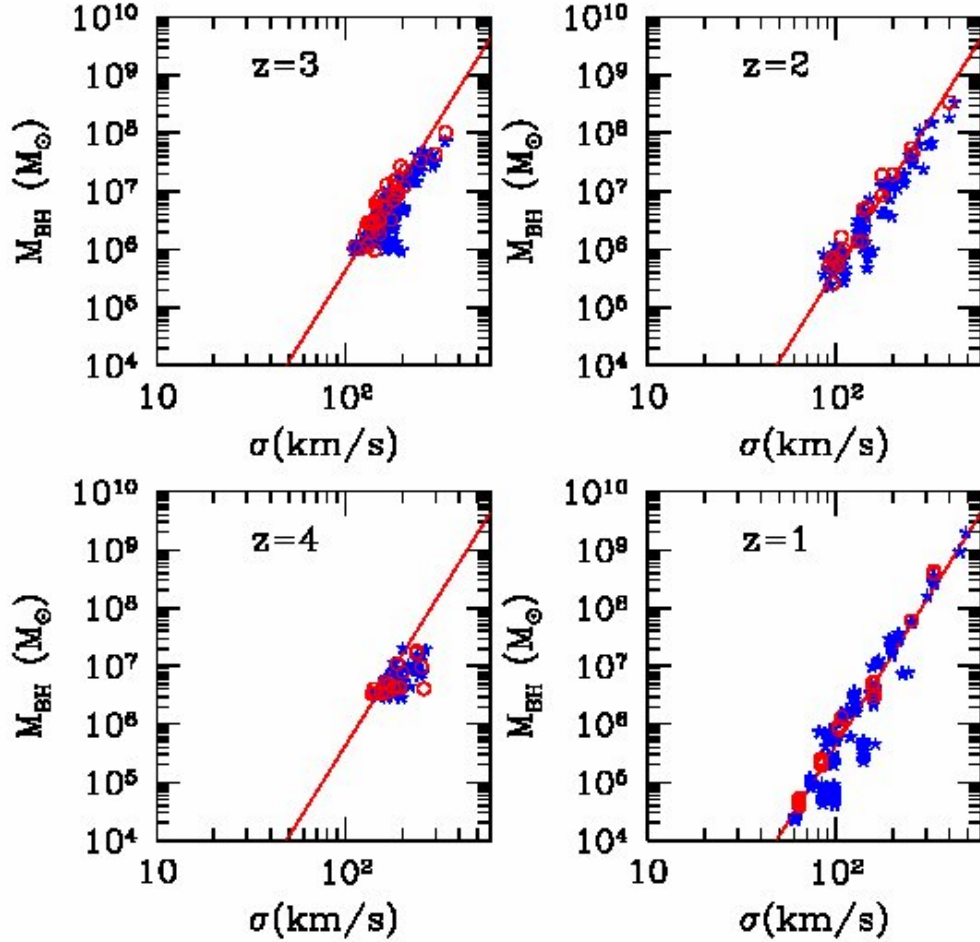


FIGURE 6. The $M_{\text{BH}} - \sigma$ relation for active MBHs at different redshift slices in the ET progenitors. These MBHs would be observed as AGNs. We imposed a flux threshold, $10^{-16} \text{ erg s}^{-1} \text{ cm}^{-2}$ (bolometric). Stars: Massive seeds based on the model by Lodato & Natarajan (2006), with $Q_c = 2$. Circles: seeds based on Population III star remnant models (Volonteri et al. 2003). The figure shows both central and satellite MBHs (satellite holes are shown at the σ of the host halo). The sample comprises all the progenitors of 20 $z = 0$ halos.

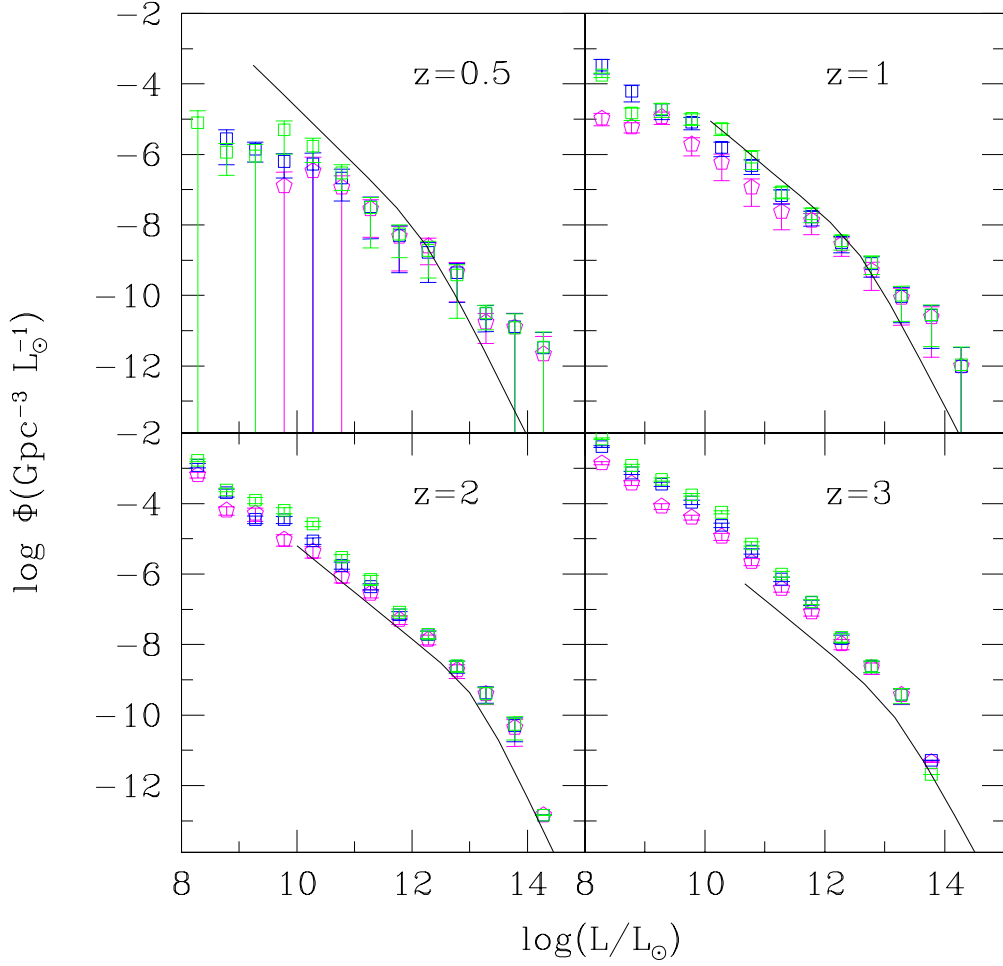


FIGURE 7. Predicted bolometric luminosity functions at different redshifts with observational data over-plotted. All 3 models match the observed bright end of the LF at high redshifts and predict a steep slope at the faint end down to $z = 1$. The 3 models are not really distinguishable with the LF. However at low redshifts, for instance at $z = 0.5$, all 3 models are significantly flatter at both high and low luminosities and do not adequately match the current data. As discussed in the text, the LF is strongly determined by the accretion prescription and what we see here is simply a reflection of that fact.

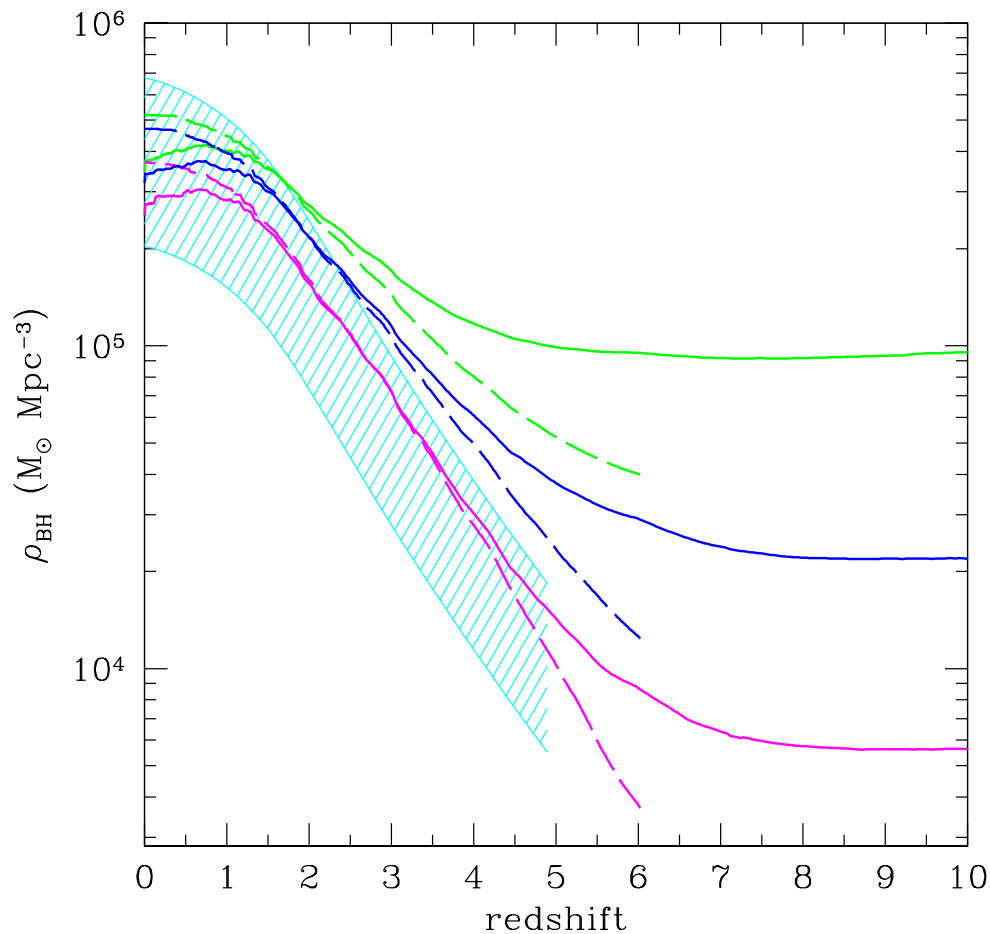


FIGURE 8. Integrated black hole mass density as a function of redshift. Solid lines: total mass density locked into nuclear black holes. Dashed lines: integrated mass density accreted by black holes. Models based on BH remnants of Population-III stars (lowest curve), $Q_c = 1.5$ (middle lower curve), $Q_c = 2$ (middle upper curve), $Q_c = 3$ (upper curve). Shaded area: constraints from Soltan-type arguments, where we have varied the radiative efficiency from a lower limit of 6% (applicable to Schwarzschild MBHs, upper envelope of the shaded area), to about 20%. All 3 massive seed formation models are in comfortable agreement with the mass density obtained from integrating the optical luminosity functions of quasars.

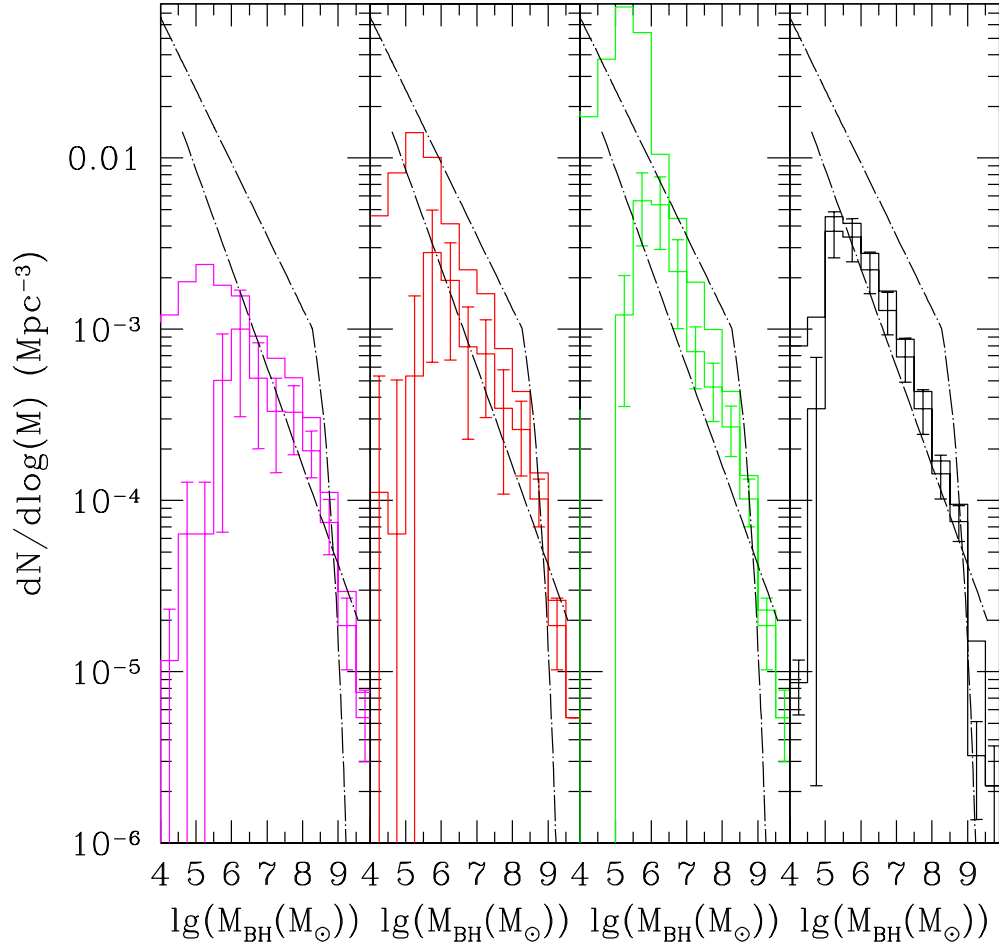


FIGURE 9. Mass function of black holes at $z=0$. Histograms represent the results of our models, including central galaxies only (lower histograms with errorbars), or including satellites in groups and clusters (upper histograms). Left panel: $Q_c = 1.5$, mid-left panel: $Q_c = 2$, mid-right panel: $Q_c = 3$, right panel: models based on BH remnants of Population-III stars. Upper dashed line: mass function derived from combining the velocity dispersion function of Sloan galaxies (Sheth et al. 2003, where we have included the late-type galaxies extrapolation), and BH mass-velocity dispersion correlation (e.g., Tremaine et al. 2002). Lower dashed line: mass function derived using the Press-Schechter formalism from Jenkins et al. (2001) in conjunction with the $M_{\text{BH}} - \sigma$ relation (Ferrarese 2002).